The Astrophysical Journal, 614:1022–1027, 2004 October 20

A MODEL FOR BRIGHT EXTREME-ULTRAVIOLET KNOTS IN SOLAR FLARE LOOPS

S. Patsourakos,[1] S. K. Antiochos, and J. A. Klimchuk
Naval Research Laboratory, Space Science Division, Washington, DC 20375; patsourakos@nrl.navy.mil
Received 2004 March 1; accepted 2004 June 25

ABSTRACT

EUV observations often indicate the presence of bright knots in flare loops. The temperature of the knot plasma is of the order of 1 MK, and the knots themselves are usually localized somewhere near the loop tops. We propose a model in which the formation of EUV knots is due to the spatial structure of the nonflare active region heating. We present the results of a series of one-dimensional hydrodynamic, flare-loop simulations, which include both an impulsive flare heating and a background, active region heating. The simulations demonstrate that the formation of the observed knots depends critically on the spatial distribution of the background heating during the decay phase. In particular, the heating must be localized far from the loop apex and have a magnitude comparable to the local radiative losses of the cooling loop. Our results, therefore, provide strong constraints on both coronal heating and postflare conditions.

Subject headings: hydrodynamics — Sun: corona — Sun: flares — Sun: UV radiation

Online material: color figure

1. INTRODUCTION

Solar flares represent gigantic releases of energy, 10^{32} ergs or more in a matter of a few minutes, with dramatic manifestations over large domains of the electromagnetic spectrum (e.g., Tandberg-Hanssen & Emslie 1988). The standard model for flare energy release is based on the magnetic reconnection of oppositely directed flux (e.g., Carmichael 1964; Sturrock 1966; Hirayama 1974; Kopp & Pneuman 1976; Heyvaerts et al. 1977). In this model, field lines that were opened by an eruption close down and form the hot flare loops visible in soft X-rays (e.g., Kopp & Pneuman 1976). Initially, the flare loops have temperatures of tens of MK, but then they start to cool down to coronal temperatures.

A self-consistent treatment of magnetic reconnection with plasma energy losses that include radiation and thermal conduction is a daunting task in a full three-dimensional geometry. Therefore, many authors have studied, instead, one-dimensional hydrodynamic flare loop models (for a review see Bray et al. 1991). In the majority of the models the heating in the decay phase of the flare is assumed to return to a preflare state in which the heating is spatially uniform. However, from a series of recent theoretical (Antiochos et al. 1999, 2000b; Karpen et al. 2001; Gudiksen & Nordlund 2002; Priest et al. 2002; Schrijver & Title 2002; Müller et al. 2003) and observational studies (e.g., Aschwanden et al. 2001; Vlahos & Georgoulis 2004) a new paradigm has emerged for coronal heating. According to this paradigm the quasi-steady heating is likely to be spatially localized near the footpoints of coronal loops. It should be emphasized, however, that this new paradigm is by no means universally accepted.

One of the most conspicuous features of flare loops observed in the extreme-ultraviolet (EUV) is the presence of bright emission "knots" along them (e.g., Cheng 1980; Dere et al. 1977; Widing & Hiei 1984; Golub et al. 1999; Warren 2000). In Figure 1 we show several examples of these knots. The images were taken by the *Transition Region and Coronal Explorer* (*TRACE*; Handy et al. 1999) in an EUV channel centered around 173 Å, which is most sensitive to plasmas at $\sim$1 MK. As is evident from Figure 1, knots can be found in flare loops seen in both the disk and the limb. The 173 Å knots are typically 2–4 times brighter than the rest of the loop, although contrasts as large as 10 can be found. They exhibit proper motions of a few 10 km s^{-1}. Their lifetime (defined as the time the knots are visible in the 173 Å channel) varies between roughly 1 and 10 minutes. The key issue that we address in this paper is the physical origin of these emission inhomogeneities in flare loops. One possible cause is line-of-sight effects in the optically thin corona (Alexander & Katsev 1996). A coronal loop with a complex three-dimensional geometry may well appear brighter in sections where the line of sight is parallel to the loop axis. However, it seems unlikely that such an effect can account for the knots seen at the disk center, where the loop geometry appears to be well determined. Another possibility is that the loop cross section is larger at the locations of knots; however, this model also seems unlikely given the fact that multiple knots often occur along flare loops. In this case the loop would have to have a rather "exotic" geometry with an undulating cross section along its length. Moreover, we have found that as in our results on quiet loops, EUV flare loops do not exhibit significant cross-sectional expansion with height (Watko & Klimchuk 2000). Finally, the fact that the knots are moving along the loops seems to invalidate the possibility that they are formed by the magnetic trapping of plasma condensations formed by reconnection at the loop top.

Antiochos (1980) proposed that the Hα knots observed in the late cooling phase of large two-ribbon flares, the so-called loop prominence systems (Bruzek 1964), are due to a type of thermal instability. He found that if an initially hot, 10^7 K, flare loop had a perturbation in its temperature and density profiles such that the temperature exhibited a slight minimum near the loop apex, then this minimum would grow to form an Hα condensation well before the rest of the loop cooled to chromospheric temperatures. Even a perturbation of only 5% amplitude was sufficient to lead to runaway cooling and to an Hα knot that lived for tens of minutes (Antiochos 1980).

[1] Also at: Center for Earth Observing and Space Research, Institute for Computational Sciences, George Mason University, Fairfax, VA 22030.

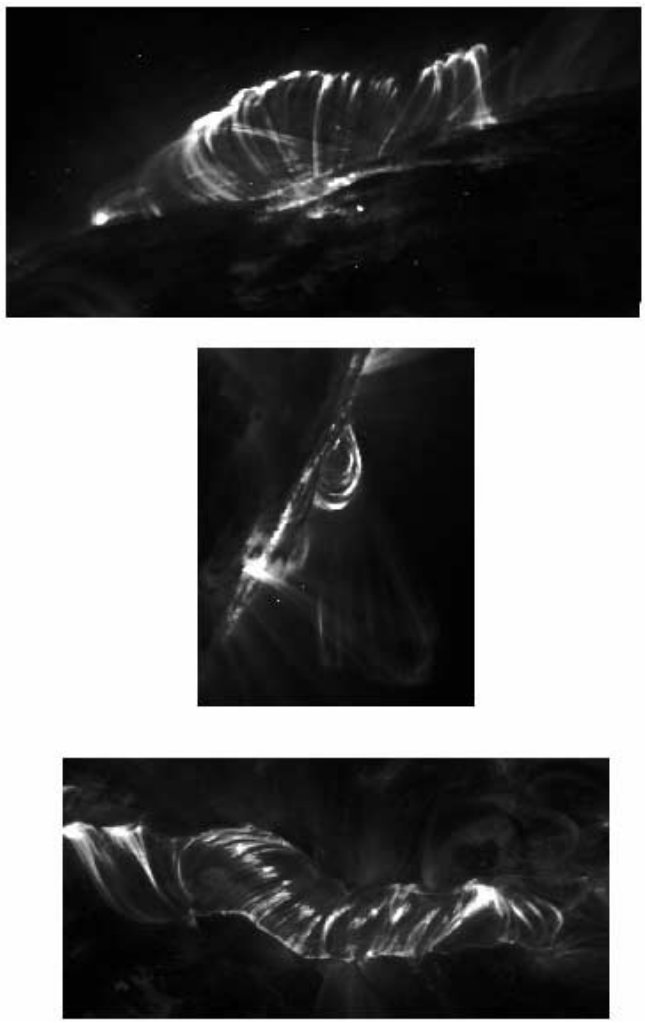

FIG. 1.—Examples of knots in postflare loops seen in the 173 Å channel of *TRACE*. [*See the electronic edition of the Journal for a color version of this figure.*]

We propose that a similar process may be responsible for the EUV knots seen by *TRACE* during the cooling phase of flare loops. The key question, however, is why the temperature develops a minimum near the loop apex. In our previous work (Antiochos 1980), the existence of the minimum was simply assumed. In this paper, we argue that the temperature inversion is formed by a background coronal heating that is localized away from the loop apex. Such a spatial dependence is unlikely to be valid for flare heating, which in the standard model is believed to be due to reconnection at a vertical current sheet above the observed loops. However, as discussed above, there have been numerous results recently indicating that the quasi-steady heating in nonflare coronal loops is concentrated near the chromosphere. We conjecture that although this heating is insufficient to maintain the loop plasma at the high temperatures produced by a flare, the quasi-steady heating is sufficient to create a temperature minimum near the top after the flare has shut off and the loop material begins to cool down. Once created, this minimum will then grow to form the knots seen in EUV and eventually Hα. If this model is correct, then the observed properties of the knots may be used to place constraints on active region heating. In this paper, we investigate our model for the formation of EUV knots in flare loops with detailed numerical simulations.

The paper is organized as follows: in § 2 we describe the numerical code and list the different models considered in this study, and in § 3 we present the results of our simulations. This paper concludes in § 4 with a discussion of the implications of our results.

2. NUMERICAL MODEL

The one-dimensional time-dependent hydrodynamic equations for a coronal loop with constant cross section were solved using our state-of-the-art adaptive mess refinement code called ARGOS. For more technical details on ARGOS the reader is referred to Antiochos et al. (2000b). For the simulations reported in this paper we assume that the heating function $H(s, t)$ is separable in position along the loop s and time t, and express it as:

$$H(s, t) = h(s)g(t). \quad (1)$$

For the loop geometry we assume a constant cross section flux tube with total length L of 164,000 km. The loop includes two long chromospheric sections of length 60,000 km each, which provides an ample reservoir of mass for chromospheric evaporation and places the bottom boundary conditions sufficiently far that they have no effect on the coronal evolution. The coronal section of the loop consists of a semicircle that is oriented vertically to the solar surface and is 44,000 km long (including a thin transition region at the bottom). Therefore, our coronal loop has a half-length $L_{1/2}$ of 22,000 km, and its apex is situated initially at a height of $\sim$14,000 km above the top of the chromosphere. The position of the top of the chromosphere moves downward during the impulsive heating phase because of the increase of plasma pressure in the coronal section of the loop during this phase. The locations of the initial position of the top of the chromosphere in each loop leg are given by s_1 and $L - s_1$.

As initial conditions for our flare simulations, we constructed an equilibrium loop solution for a spatially uniform, steady state heating rate $\epsilon_0 = 0.005$ ergs cm^{-3} s^{-1}. The code was run for a sufficient time ($\sim$60,000 s), corresponding to several sound transit times along the loop, so that the system relaxed to a true, static equilibrium with negligible residual mass motions ($<$0.2 km s^{-1}) and with an apex temperature and density of $\sim$2.7 MK and 3.3×10^9 cm^{-3}, respectively. All the numerical simulations described below use this solution as the initial state of the loop at $t = 0$ s. It should also be noted that the form of the heating and the details of the plasma structure before the flare are essentially irrelevant to the subsequent evolution, because the impulsive heating is so much larger than the preflare heating.

We then subject this initial equilibrium state to two forms of time-dependent heating, referred to as the "uniform" and "localized" heating models. For both models we assume a temporal dependence for the heating during the flare impulsive phase $g(t)$ that has the form of a step function with a duration of 300 s. This assumption corresponds to an instantaneous turn-on of flare heating, which appears to agree with several observations (e.g., Antiochos et al. 2000a). Furthermore the heating during the impulsive phase is assumed to be concentrated at the loop apex, thereby mimicking thermal models of flares. The spatial scale σ for $h(s) = \epsilon_1 \exp[-(s - L/2)/\sigma]$ of equation (1) is assumed be 1000 km, which corresponds to 1/22 of the initial half-length $L_{1/2}$ of the coronal section of the loop. In any case, since we are interested only in the late phases of plasma cooling, the details of $g(t)$ and $h(s)$ during the

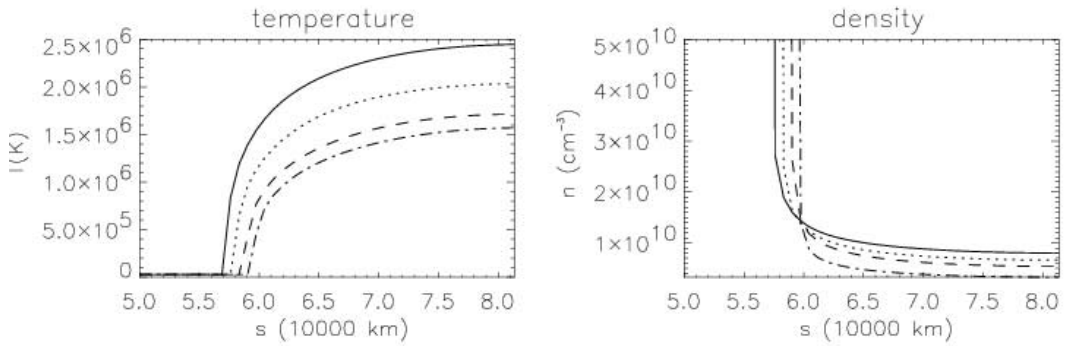

FIG. 2.—Snapshots of the temperature and density as a function of the position along the loop for the uniform heating model. Curves show times from $t = 0$: *solid*, 1399 s; *dotted*, 1599 s; *dashed*, 1800 s; *dash-dotted*, 2299 s.

impulsive phase are not expected to have a significant effect on our results. Finally, the applied heating ϵ_1 during the impulsive phase is 1000 times larger than its preflare (spatially uniform) value ϵ_0, which implies that the total heating rate over the entire loop length increases by a factor of about 50 during the flare. The maximum temperature in the loop reaches 12 MK, in agreement with typical flare loop temperatures.

During the decay phase the temporal dependence of the heating $g(t)$ is set to unity for both models, but the spatial dependence is very different. For the uniform model (§ 3.1) we assume that the loop heating returns to a spatially constant state with magnitude equal to the preflare value ϵ_0. For the localized model (§ 3.2), on the other hand, we assume a background heating that is concentrated toward the loop footpoints, $h(s) = \epsilon_1 \exp[-(s - s_1)/\sigma]$ for $s_1 \le s < s_1 + L_{1/2}$ with $\sigma = 1000$ km, and $h(s) = \epsilon_1$ for $s < s_1$. The heating is assumed to be symmetric around the loop apex, i.e., $h(s) = \epsilon_1 \exp\left[-(s_1 + 2L_{1/2} - s)/\sigma\right]$ for $s_1 + L_{1/2} \le s \le s_1 + 2L_{1/2}$ and $h(s) = \epsilon_1$ for $s > s_1 + 2L_{1/2}$. Because of the imposed symmetry we show results from the one half of the loop in § 3 for the two models. The magnitude of the localized model heating is chosen so that the total heating in the loop returns to its preflare value, $\epsilon_1 = 22\epsilon_0$. In summary, the two cases have identical initial states, flare heating, and total background heating, but differ in the spatial dependence for the background heating.

3. RESULTS

For the two cases described above, we obtained solutions to the one-dimensional hydrodynamic problem by using ARGOS to calculate the density, temperature, and flow velocity as a function of time and position along the loop. Given the calculated temperature $T(s, t)$ and density $n(s, t)$ distributions, we were then able to calculate the signal $S_{TR}(s, t)$ that *TRACE* would detect at position s and time t from the simulated loops,

$$S_{TR}(s, t) = [n(s, t)]^2 G_{TR}(T(s, t))\, dl, \qquad (2)$$

where $G_{TR}(T)$ is the temperature response for any given *TRACE* channel expressed in units of data numbers (DN) per pixel per second per unit column emission measure, and dl is the integration length across the loop. We use for dl a constant value of 2000 km over the entire loop length, since our loops are assumed to have constant cross section. Furthermore we assume that the loops are observed face-on. In this work we show the signal for the 173 Å channel of *TRACE*. Equation (2) indicates that the signal and thus the loop morphology that *TRACE* would see at any given time is a function of the temperature and density distribution along the loop; therefore, it is clear that in order to obtain emission knots, $T(s, t)$ and/or $n(s, t)$ must have bumps and peaks along the loop, i.e., they must be nonmonotonic.

3.1. *Uniform Background Heating*

In Figure 2 we plot temperature and density profiles along the loop for the uniform model. They correspond to several times during the late stages of the cooling when the coronal temperatures are in the range ~0.65–2.5 MK. It is evident that both density and temperature along the cooling loop are smooth and monotonic without any local extrema, indicating that EUV knots are not formed for this case.

The physical origin for this result can be understood from the following arguments. Since the flare heating is localized at the loop midpoint, it raises the local temperature to produce a strong maximum at the midpoint, irrespective of the initial temperature profile in the loop. Once the flare heating turns off, the initial cooling is dominated by thermal conduction, which acts to set up a temperature profile that is monotonically decreasing from this temperature maximum down to the low-temperature chromospheric footpoints. Note also that even if the flare heating is localized at some position away from the midpoint, resulting in a temperature maximum that is off to one side of the loop, conduction cooling will establish a maximum at the midpoint, once the heating turns off. Since the timescale for conductive cooling τ_c depends strongly on the distance from the temperature maximum to the chromosphere, $\tau_c \propto L^2$, the short side will cool faster than the long side, thereby moving the temperature maximum toward the midpoint. We expect, therefore, that an impulsively heated flare loop will generally begin its radiative cooling phase with a temperature profile that has a single maximum midpoint from the two chromospheric footpoints.

The question now is whether condensations (or local minima) can form during the radiative phase. This appears likely, because a radiatively dominated plasma is subject to the well-known thermal instability (e.g., Field 1965). Of course, the concept of a thermal instability is not strictly applicable to a cooling loop, because the system is fully time dependent and never in equilibrium. However, it is certainly possible to consider the situation in which the loop cools unevenly, so that a part of the loop plasma cools down to the *TRACE* temperature range well before the rest of the loop. If so, this would appear as a condensation. The obstacle to forming a condensation, however, is that for an isobaric loop at flare temperatures the radiative loss rate is a strongly decreasing function of

temperature. Therefore, we expect that radiative cooling in a flare loop will be weakest at the temperature maximum and strongest in the transition region near the footpoints, which acts only to enhance the maximum in the corona. In order for thermal instability to produce a condensation, the temperature profile at the onset of radiative cooling must have a local minimum somewhere in the corona (e.g., Antiochos 1980). It is possible that, because of the presence of evaporation and other strong dynamics during the heating and initial cooling phase, local temperature minima form in the corona, but these generally propagate along the loop and are damped out quickly by conduction well before the onset of radiative cooling. Therefore, radiative cooling by itself is unlikely to produce a condensation in a flare loop. Some other mechanism is required to produce the local temperature minimum that is required to seed the instability.

As the loop cools by radiation, the temperature and hence the gravitational scale height decrease, resulting in material draining down the legs. This loss of density decreases the radiative loss rate until eventually the background heating can have a noticeable effect on the evolution. In principle, the background heating could act to produce a local temperature minimum, but it fails to do so for two reasons. First, the heating is spatially constant in the uniform model; hence, it simply decreases the effective cooling rate by a fixed amount everywhere. Consequently, the arguments above still hold—the effective cooling rate increases toward the loop footpoints, enhancing the temperature maximum at the midpoint. Second, the background heating is too small compared to the radiative cooling rate to have a noticeable effect. Before the flare, we expect that the heating rate and radiative cooling rate in the coronal portion of the loop are approximately equal, as is given by the well-known loop scaling laws (e.g., Rosner et al. 1978; Vesecky et al. 1979). As a result of the flare heating, the density in the loop increases by over an order of magnitude, which implies that the cooling rate at the onset of the radiative phase is over 2 orders of magnitude larger than its preflare value and hence larger than the background heating by the same factor. Of course as the loop cools and material drains, the density and radiative rate decrease. Using now the result found by Cargill et al. (1995) that the density of a cooling flare loop decreases only as the square root of the loop temperature, and assuming that the radiative losses function scales as $T^{-1/2}$, we find that the radiative cooling rate varies as $T^{1/2}$. This indicates that the radiative cooling rate decreases only by a factor of 3 or so as the loop cools from 10^7 K to the *TRACE* temperature band. Consequently, the background heating is negligible compared to the radiative cooling rate, even when the loop reaches the *TRACE* temperatures, and is unlikely to affect the form of the temperature profile. We conclude from this discussion that a cooling flare loop with a uniform background heating will have a monotonic temperature profile throughout its evolution and thus will not develop condensations.

3.2. *Localized Background Heating*

In Figure 3 we plot temperature, density, and velocity along the loop for the localized model, again during the late stages of cooling as in Figure 2 for the uniform case. It is evident that in this case the temperature and density profiles are far from monotonic. For the first time shown, the temperature still has its maximum at the loop apex, but a local minimum is starting to develop just above the region of localized heating. The reason is that, near the footpoints, the heating rate can be a factor of 22 larger than the uniform value above. Consequently, the background heating eventually becomes significant compared to the radiative cooling near the footpoints. This decreases the effective cooling there so that by the time that the flare plasma has dropped down to the *TRACE* temperatures, the effective cooling rate is no longer monotonically increasing from the midpoint. It has a maximum somewhere just above the localized heating region, which drives the formation of a local temperature minimum. Once this minimum forms, the thermal instability then takes over and a condensation rapidly develops. We note that the density has a local maximum where the temperature is minimum.

Figure 3 shows the early stages of the condensation formation, when the temperatures are still within the *TRACE* passband. Because of the strong density dependence of the radiative loss rate, the cooling timescale becomes very short, of the order of 100 s, as the temperature drops below 10^6 K. We found the same behavior in all our loop simulations that involved the formation of a condensation (the Antiochos et al. 2000b; Karpen et al. 2001, 2003 thermal nonequilibrium papers). It is clearly evident from Figure 3 that the temperature minimum moves to the right with time. One generally expects such a minimum to grow in place as material flows in from both sides to counter the rapid pressure decrease there. However, for this nonuniform heated loop the plasma pressure drops more slowly in the region of localized heating than in the rest of the loop. This sets up a strong pressure gradient from the footpoints to the midpoint, which drives a substantial flow up the loop. By the last time shown, the velocities have reached almost 40 km s^{-1}. In fact, during the final stages of the evolution when the condensation reaches Hα temperatures and collapses onto the midpoint, rebound shocks can be seen in the simulation. Again, this evolution is in good agreement with previous calculations of condensation formation.

In Figure 4 we plot the signal along the loop in the 173 Å channel of *TRACE* for the six times shown in Figure 3. Only the upper portion of the loop, $s > 6 \times 10^4$ km, is shown so as to eliminate the intense emission from the footpoints, the so-called flare moss (Antiochos et al. 2000a). At early times the emission in 173 Å is negligible in the corona portion of the loop, because the temperatures there are too high, but it is large at the 10^6 K flare transition region. If we take arbitrarily 10 DN $pixel^{-1}$ s^{-1} as the minimum signal observable by *TRACE*, then the loop does not become visible until around $t = 1600$ s. It is interesting to note that the intensity maximum does not coincide with either the locations of the density or temperature peaks, although it tends to be close to the density peak. This is a result of the contribution function for the *TRACE* signal, which spans a broad temperature range ($\sim$0.65–1.15 MK) and is weighted by the square of density (eq. [2]).

The key result of Figure 4 is that the structure and evolution of the 173 Å signal is quite complex. This is very different from the uniformly heated case, in which the emission is first visible at the loop footpoints and then smoothly increases upward to fill the whole loop. In the nonuniform case the emission first appears somewhere in the loop legs and fills a large fraction of the loop, but there is a clear gap in emission between the footpoints and the location of strong signal. Hence, *TRACE* would observe only a partial loop, very similar to the observations shown in Figure 1. We note that after $t = 1610$ s a "knot" forms at $\sim s = 6.6 \times 10^4$ km and moves first toward larger s, until $\sim t = 1710$ s, and then toward lower s, with an apparent speed of $\sim$10–20 km s^{-1}. Such moving intensity fronts are often seen in postflare loops observed by *TRACE*. The knot is brighter than its surroundings by a factor of up to

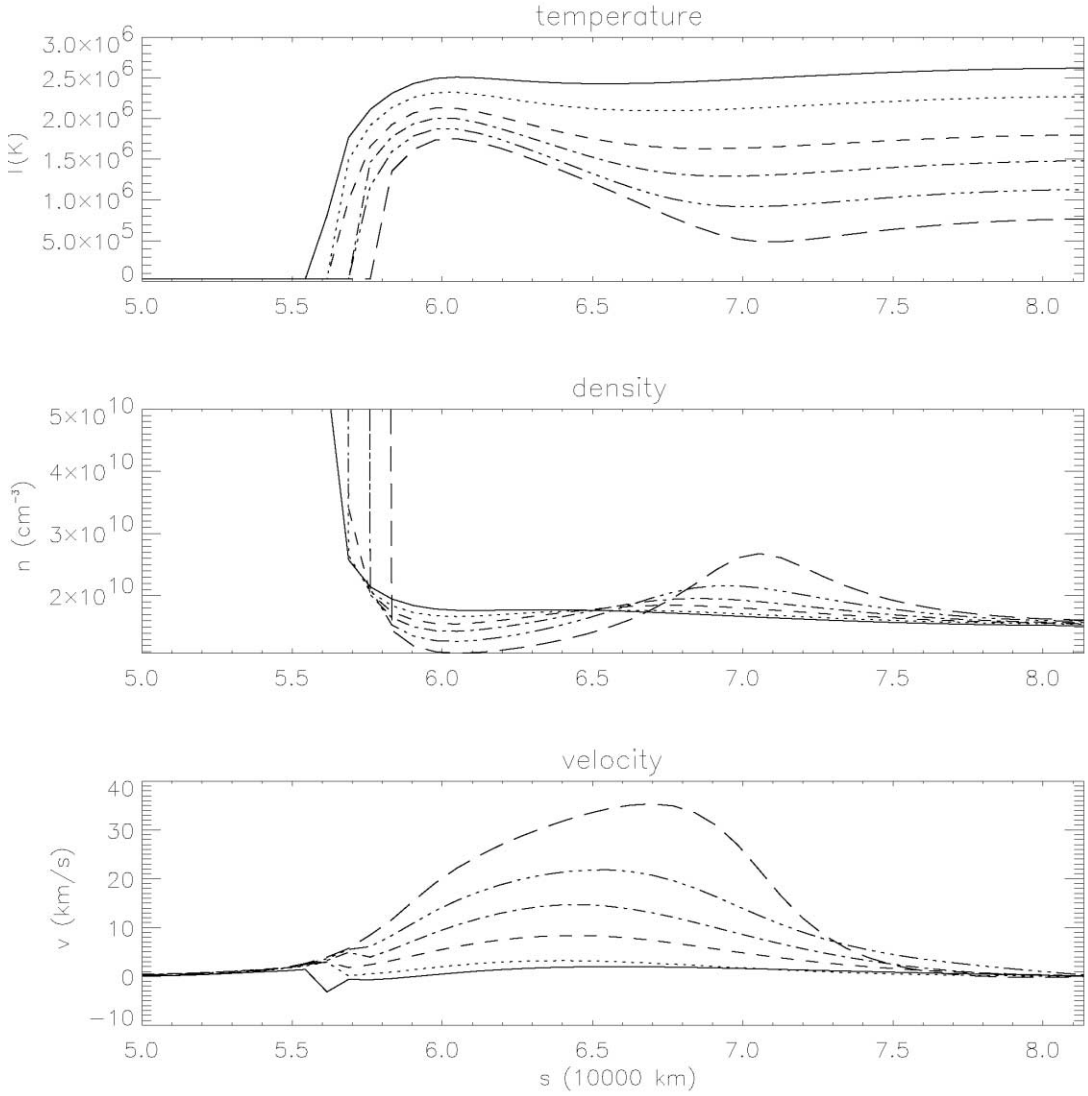

FIG. 3.—Snapshots of the temperature (*top panel*), density (*middle panel*), and velocity evolution (*bottom panel*) along the loop for the localized heating model. Curves show times from $t = 0$: *solid*, 1410 s; *dotted*, 1509 s; *dashed*, 1610 s; *dash-dotted*, 1660 s; *dash-triple dotted*, 1710 s; *long dashed*, 1760 s. Positive velocities correspond to upflows.

$\sim$3 and has a lifetime of the order of 250 s. It has a FWHM in the range $\sim$5000–10,000 km, which corresponds to a significant fraction of the total length of the coronal section of the loop. Although we have not attempted to fit any particular observation with this simulation, it seems evident that the structure and complexity of the resulting signal is much more likely to fit the observations of Figure 1 than in the uniformly heated case.

4. DISCUSSION AND CONCLUSIONS

The main conclusion of § 3 is that the formation of knots in EUV postflare loops requires a specific form for the background quasi-steady heating in the active region. Our results thus place strong constraints on the properties of the background quasi-steady heating. The heating cannot be either uniform or localized toward the loop apex for the knots to form, because in both cases the temperature of the cooling loop would be monotonic. In fact when the background active region heating is located near (or at) the loop apex, the apex cools down even slower with respect to the rest of the loop as compared to the case of no or uniform background heating. This obviously maintains a monotonic temperature profile throughout the cooling loop, with the temperature decreasing from the apex. The spatial length σ of the localized background heating cannot be larger than a sizable fraction of the loop half-length. Otherwise, the heating would be more or less uniform along the loop and no knots would form. It seems likely that σ does not strongly depend on the loop length, because *TRACE* flare movies taken near the limb seem to indicate that knots are mainly formed in the high-arching postflare loops. This means that σ could be comparable to the length of the shorter loops, therefore implying a more or less uniform heating in those loops, which does not favor knot formation. Modifying σ would shift the initial position of the knot along the loop closer to (when σ increases) or farther from (when σ decreases) the loop apex. Furthermore, increasing or decreasing the magnitude of the background heating would lead to knot formation earlier or later during the cooling of the flare loop, respectively.

In our calculations we assumed that the background localized heating was symmetric. However, perfect symmetry conditions should be rare on the real Sun and therefore the background quasi-steady active region heating can be asymmetric.

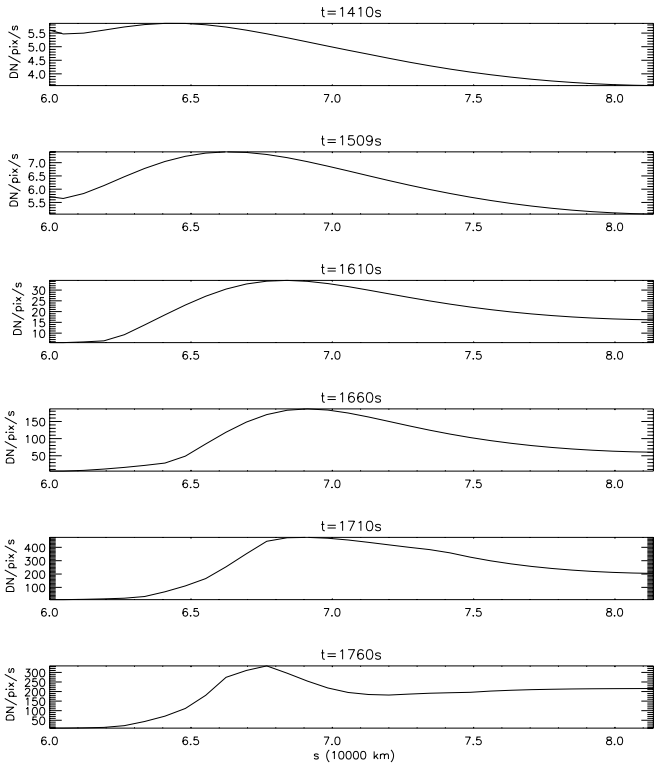

FIG. 4.—Snapshots of the synthesized *TRACE* signal in the 173 Å channel as a function of position along the loop for the localized heating model. These snapshots correspond, from the top to the bottom panel, to times 1410, 1509, 1610, 1660, 1710, and 1760 s from $t = 0$.

Asymmetric heating is prone to lead to more complex loop dynamics, similar to the formation of condensations in prominence loops (e.g., Antiochos et al. 2000b; Karpen et al. 2001). As we have seen before condensations in prominence loops are also formed when the heating is concentrated toward the chromosphere. However, in the case of postflare loops the applied background heating perturbs an evolving cooling loop. Moreover the timescales for the formation of condensations and their lifetimes are significantly larger for prominence loops as compared to postflare loops given the enhanced densities associated with postflare loops.

In § 3.2 we assumed that the localized heating is concentrated toward the chromospheric sections of the modeled loop. This choice, however, is by no means the only one capable of producing condensations. As discussed above and in § 3.2, all that matters for condensations to form is that the heating is localized away from the loop apex, so that local temperature minima appear. We verified the above conjecture by running flare-loop simulations with the heating during the decay phase, parametrized by a Gaussian profile with a width of $\sim$1000 km, localized at various locations along the coronal section of the loop. We found that even when this heating is localized halfway from the top of the chromosphere to the apex, condensations and thus EUV knots form. By using a similar heating profile Antiochos & Klimchuk (1991) perturbed an equilibrium loop and found that it leads to the formation of prominence condensations.

Our conclusion that the quasi-steady coronal heating must be localized is fully consistent with a bulk of recent independent observational and theoretical works described in the introduction. It is remarkable to note that the observations and modeling of seemingly different types of coronal loops (i.e., quiescent, postflare, prominence) all point to a universal scenario for the quasi-steady heating: it must be localized. However, while some of these works refer to a steady state corona (e.g., Aschwanden et al. 2001), our work corresponds to a dynamic corona, as expected when plasma cooling occurs. We emphasize that EUV knots are also seen in quiescent loops undergoing catastrophic cooling (e.g., Levine & Withbroe 1977; Schrijver 2001). It is therefore possible that a similar scenario applies to quiescent loops. Active region loops could first be impulsively heated to a few MK, and then additional localized background heating could lead to the formation of the observed knots in these loops when they cool down.

This research was supported by NASA and the Office of Naval Research. We thank J. Cook, K. Dere, G. Doschek, L. Golub, J. Karpen, J. Mariska, and H. Warren for useful discussions and the referee for useful comments.

REFERENCES

Alexander, D., & Katsev, S. 1996, Sol. Phys., 167, 153
Antiochos, S. K. 1980, ApJ, 236, 270
Antiochos, S. K., DeLuca, E. E., Golub, L., & McMullen, R. A. 2000a, ApJ, 542, L151
Antiochos, S. K., & Klimchuk, J. A. 1991, ApJ, 378, 372
Antiochos, S. K., MacNeice, P. J., & Spicer, D. S. 2000b, ApJ, 536, 494
Antiochos, S. K., MacNeice, P. J., Spicer, D. S., & Klimchuk, J. A. 1999, ApJ, 512, 985
Aschwanden, M. J., Schrijver, C. J., & Alexander, D. 2001, ApJ, 550, 1036
Bray, R. J., Cram, L. E., & Durrant, C. J. 1991, Plasma Loops in the Solar Corona (Cambridge: Cambridge Univ. Press)
Bruzek, A. 1964, ApJ, 140, 746
Cargill, P. J., Mariska, J. T., & Antiochos, S. K. 1995, ApJ, 439, 1034
Carmichael, H. 1964, in The Physics of Solar Flares, ed. W. N. Hess (NASA CP-50; Washington: NASA), 451
Cheng, C. C. 1980, Sol. Phys., 65, 347
Dere, K. P., Horan, D. M., & Kreplin, R. W. 1977, ApJ, 217, 976
Field, G. B. 1965, ApJ, 142, 531
Golub, L., et al. 1999, Phys. Plasmas, 6, 2205
Gudiksen, B. V., & Nordlund, A. 2002, ApJ, 572, L113
Handy, B. N., et al. 1999, Sol. Phys., 187, 229
Heyvaerts, J., Priest, E. R., & Rust, D. M. 1977, ApJ, 216, 123
Hirayama, T. 1974, Sol. Phys., 34, 323
Karpen, J. T., Antiochos, S. K., Klimchuk, J. A., & MacNeice, P. J. 2003, ApJ, 593, 1187
Karpen, J. T., et al. 2001, ApJ, 553, L85
Kopp, R. A., & Pneuman, G. W. 1976, Sol. Phys., 50, 85
Levine, R. H., & Withbroe, G. L. 1977, Sol. Phys., 51, 83
Müller, D. A. N., Hansteen, V. H., & Peter, H. 2003, A&A, 411, 605
Priest, E. R., Heyvaerts, J. F., & Title, A. M. 2002, ApJ, 576, 533
Rosner, R., Tucker, W. H., & Vaiana, G. S. 1978, ApJ, 220, 643
Schrijver, C. J. 2001, Sol. Phys., 198, 325
Schrijver, C. J., & Title, A. M. 2002, Sol. Phys., 207, 223
Sturrock, P. A. 1966, Nature, 211, 695
Tandberg-Hanssen, E., & Emslie, A. G. 1988, The Physics of Solar Flares (Cambridge: Cambridge Univ. Press)
Vesecky, J. F., Antiochos, S. K., & Underwood, J. H. 1979, ApJ, 233, 987
Vlahos, K., & Georgoulis, M. K. 2004, ApJ, 603, L61
Warren, H. P. 2000, ApJ, 536, L105
Watko, J. A., & Klimchuk, J. A. 2000, Sol. Phys., 193, 77
Widing, K., & Hiei, E. 1984, ApJ, 281, 426